



# A seesaw in Mediterranean precipitation during the Roman Period linked to millennial-scale changes in the North Atlantic

B. J. Dermody<sup>1</sup>, H. J. de Boer<sup>1</sup>, M. F. P. Bierkens<sup>2</sup>, S. L. Weber<sup>3</sup>, M. J. Wassen<sup>1</sup>, and S. C. Dekker<sup>1</sup>

<sup>1</sup>Department of Environmental Sciences, Copernicus Institute of Sustainable Development, Utrecht University, The Netherlands

<sup>2</sup>Department of Physical Geography, Utrecht University, The Netherlands

<sup>3</sup>Royal Netherlands Meteorological Institute (KNMI), De Bilt, The Netherlands

Correspondence to: B. J. Dermody (b.dermody@uu.nl)

Received: 17 June 2011 – Published in *Clim. Past Discuss.*: 14 July 2011

Revised: 20 February 2012 – Accepted: 28 February 2012 – Published: 29 March 2012

**Abstract.** We present a reconstruction of the change in climatic humidity around the Mediterranean between 3000–1000 yr BP. Using a range of proxy archives and model simulations we demonstrate that climate during this period was typified by a millennial-scale seesaw in climatic humidity between Spain and Israel on one side and the Central Mediterranean and Turkey on the other, similar to precipitation anomalies associated with the East Atlantic/West Russia pattern in current climate. We find that changes in the position and intensity of the jet stream indicated by our analysis correlate with millennial changes in North Atlantic sea surface temperature. A model simulation indicates the proxies of climatic humidity used in our analysis were unlikely to be influenced by climatic aridification caused by deforestation during the Roman Period. That finding is supported by an analysis of the distribution of archaeological sites in the Eastern Mediterranean which exhibits no evidence that human habitation distribution changed since ancient times as a result of climatic aridification. Therefore we conclude that changes in climatic humidity over the Mediterranean during the Roman Period were primarily caused by a modification of the jet stream linked to sea surface temperature change in the North Atlantic. Based on our findings, we propose that ocean-atmosphere coupling may have contributed to regulating Atlantic Meridional Overturning Circulation intensity during the period of analysis.

## 1 Introduction

How human civilisation will adapt to future climate change caused by natural and anthropogenic forcings is an issue of extensive research and intense debate (IPCC, 2007). However, climate change is nothing new for human civilisation and much can be learned from understanding how past societies responded to changes in climate. One of the most advanced and enduring societies were the Romans who existed for almost 1000 yr in the Central Mediterranean during a period when climate oscillated between relatively cool and warm phases (Bianchi and McCave, 1999; Desprat et al., 2003). The Roman economy was highly integrated throughout the Mediterranean (Erdkamp, 2005) and was based primarily on agricultural production (Horden and Purcell, 2000) that was adapted to the water-limited nature of the region (Zhang and Oweis, 1999). Thus, to understand how the Romans adapted to climate change it is also important to build a picture of the change in precipitation around the Mediterranean during the Roman Period (RP) (ca. 2500–1500 yr BP). We focus our analysis on the period 3000–1000 yr BP to capture the change in climate leading up to and following the RP. Already a number of studies have provided evidence that changes in precipitation during the RP were influenced by changes in the pathway of the zonal storm tracks from the North Atlantic (Enzel et al., 2003; Jones et al., 2006; Rimbu et al., 2003). It is also proposed that large-scale deforestation beginning in the RP caused the climate around the Mediterranean to become drier as a result of a decrease in evaporative

fluxes from the land to the atmosphere (Dümenil Gates and Ließ, 2001; Reale and Dirmeyer, 2000; Reale and Shukla, 2000). Using a range of proxy archives and model simulations, we integrate these hypotheses to provide a complete regional picture of millennial-scale climate change during the RP and provide evidence of the probable forcing mechanisms responsible. It is hoped that our regional reconstruction provides a springboard for future multidisciplinary studies of the impacts of climate change on the Roman civilisation.

### 1.1 Variability in precipitation during the Roman Period

A number of proxy records provide evidence of a peak in climatic humidity in the Mediterranean during the RP. In Israel an increase in climatic humidity is apparent ca. 2000 yr BP in a speleothem record from the Soreq cave (Orland et al., 2009) and reconstructed levels of the Dead Sea (Bookman et al., 2004; Migowski et al., 2006). An isotopic analysis of trees used to construct a Roman siege ramp against Jewish rebels at the Fortress of Masada above the Dead Sea also indicate a humid peak ca. 2000 yr BP (Issar and Yakir, 1997). In Spain a reconstruction of riverine input to the Alboran Sea exhibits similar trends to lake levels from the south of the country that show a peak in climatic humidity ca. 2000 yr BP preceded and followed by relatively arid periods (Martín-Puertas et al., 2010). However, there is contrasting evidence to suggest that the period centred on 2000 yr BP was anomalously arid in certain parts of the Mediterranean. For instance, a reconstruction of climatic humidity based on fossil ostracod taxonomy and isotope analysis indicates that ca. 2000 yr BP was relatively dry around Lake Pamvotis in Greece (Frogley et al., 2001). Equally, a record of flood frequency based on pollen and charcoal analysis combined with physical indicators of floods demonstrate an anomalously dry period immediately after 2000 yr BP in Southeast Tunisia (Marquer et al., 2008). Based on  $\delta^{18}\text{O}$  values of varved lake sequences from Central Turkey, Jones et al. (2006) show that the frequency of summer droughts was greater prior to 1500 yr BP after which winter rainfall increased and summer evaporation decreased. These changes are linked to changes in the winter storm tracks over the North Atlantic but also changes in summer evaporation linked to the intensity of the Indian Monsoon (Fleitmann et al., 2003). The contrasting signals in proxy archives from around the Mediterranean highlight that the pattern of climatic change between 3000–1000 yr BP was complex. Therefore, to form a clear spatiotemporal picture of the change in climatic humidity around the Mediterranean during the period of analysis we undertake an Empirical Orthogonal Function (EOF) analysis of available proxy records. The EOF statistics highlight the dominant variability among the set of proxies and thus the dominant pattern of change in climatic humidity around the Mediterranean during the period of analysis.

Under present-day conditions the dominant mode of variability in the Mediterranean is typified by a seesaw in precipitation anomalies between the Southeast of the Mediterranean and the remainder of the basin (Düneloh and Jacobeit, 2003; Xoplaki et al., 2004). This seesaw in climatic humidity has its greatest expression in winter and is correlated with the primary mode of sea level pressure (SLP) variability over the North Atlantic: The North Atlantic Oscillation (NAO) (Barnston and Livezey, 1987; Cullen and deMenocal, 2000). Under NAO+ (NAO-) a strengthening (weakening) of the pressure gradient between a high pressure region over the Atlantic subtropics and a low near Iceland causes the track of westerly winds to move northwards (southwards), making Northern (Southern) European winters wetter and milder whilst Southern (Northern) Europe becomes drier and cooler (Barnston and Livezey, 1987; Hurrell, 1995). In the Mediterranean, NAO+ is associated with increased precipitation in the southeast whilst the remainder of the Mediterranean becomes drier with the opposite case occurring under NAO- (Cullen and deMenocal, 2000). A number of other modes of variability have also been identified in Mediterranean precipitation fields (Düneloh and Jacobeit, 2003; Xoplaki et al., 2004). The 2nd mode of variability is typified by a correlation in precipitation anomalies between the Southeast Mediterranean and the Iberian Peninsula, which are anti-correlated with the Central Mediterranean and Turkey (Xoplaki et al., 2004; Düneloh and Jacobeit, 2003). Düneloh and Jacobeit (2003) illustrate that this pattern is linked to a pressure dipole between the North Atlantic and Europe similar in structure to the East Atlantic/Western Russia pattern (EA/WR) (Barnston and Livezey, 1987).

Longer term changes in the prominent modes of climatic variability over the Mediterranean are related to the intensity and position of the zonal jet stream (Thompson and Wallace, 1998; Wallace, 2000; Ziv et al., 2006). Variations in winter climate caused by the zonal jet stream are well captured by the annular indices of climatic variability such as the Arctic Oscillation (AO). Like the NAO, the high index of the Arctic Oscillation (AO) refers to northward movement of the zonal subpolar jet and intensification of the Polar Vortex (Namias, 1950; Thompson and Wallace, 1998). The index of the AO correlates with changes in surface air temperature (SAT) in the Northern Hemisphere, particularly over the North Atlantic where it is proposed that SAT is vertically coupled to the Polar Vortex at altitude (Baldwin and Dunkerton, 1999; Cohen and Jones, 2011; Thompson and Wallace, 1998). The correlation between SAT and the annular modes is expressed by the correlation of the high phase of the AO, with anomalously warm Sea Surface Temperatures (SSTs) in the subpolar North Atlantic and cooler SSTs prevailing in the polar North Atlantic (Wallace, 2000).

In a paleo context, centennial-scale changes in the dominant modes of variability over Europe have been demonstrated in a number of studies (Büntgen et al., 2011; Cook et al., 2002; Enzel et al., 2003; Trouet et al., 2009). Trouet

et al. (2009) link centennial changes in the NAO to SST variations in the North Atlantic between 900 yr BP to present. In fact SSTs in the North Atlantic are proposed to have oscillated with a periodicity of 1450 yr known as Bond events throughout the Holocene (Bond et al., 1997, 2001). Warm intervals (cold events) of winter North Atlantic SST are inferred from a decrease (increase) in the percentage of ice rafted debris (IRD) in subpolar regions of the North Atlantic (Bond et al., 1997, 2001). Fluctuations in climate throughout the Northern Hemisphere coincident with Bond events have been indicated by a number of studies (Mayewski et al., 2004 for an overview). By comparing the dominant modes of variability identified in our EOF analysis with the periodicity of Bond events, we can explore if a coupling between Bond events and the jet stream existed that affected climate over the Mediterranean between 3000–1000 yr BP. To assist in the interpretation of land-based EOF statistics in the context of synoptic climate, we have included proxies of winter precipitation from Central and Northwest Europe in our EOF analysis so that the primary mode of variability associated with the jet stream can be identified. For example, wetter conditions in Northern Europe coincident drier conditions in the Central Mediterranean during a Bond interval would indicate a millennial coupling between North Atlantic SST and the position of the jet stream consistent with present-day correlations.

## 1.2 Anthropogenic climate change during the Roman Period

In order to fully understand climate change between 3000–1000 yr BP and the responsible mechanisms we must also consider the impact that large-scale deforestation during the RP had on climate in the Mediterranean. It is proposed that a wetter climate was maintained in the Mediterranean during the RP by greater forest cover prior to the initiation of large scale deforestation coinciding with the expansion of Roman territory (Dümenil Gates and Ließ, 2001; Reale and Dirmeyer, 2000; Reale and Shukla, 2000). The decrease in evapotranspirative fluxes and increase in albedo coinciding with an intensification of deforestation is hypothesised to have initiated a positive feedback, whereby the humid climate maintained by the biosphere became increasingly arid until it shifted to the present climate-vegetation equilibrium (Brovkin et al., 1998; Charney et al., 1975; Dekker et al., 2010). The idea that the RP was more humid compared with present has been supported, and was likely inspired by cities such as Palmyra and Petra that were populous and prosperous during the RP but are now located in desert regions (Huntington, 1911; Reale and Dirmeyer, 2000). Should the basin-wide changes in sensible and latent heat fluxes of the magnitude proposed by previous studies have occurred; it would have been imprinted on the proxy record as an aridification trend coincident with decreasing forest cover. However, such changes could be dampened by natural climate change or misinterpreted as such. Therefore we set out to isolate the

potential contribution of past anthropogenic changes on climate, using model simulations and the alternative proxy of archaeological and historical data. Therefore, we can have greater confidence that interpretations of conventional proxy records are based on the correct forcing agent.

We revisit previous studies that put forth the hypothesis that deforestation caused basin-wide climatic aridification during the RP in the Mediterranean, motivated by a number of recently published palynological and charcoal-based reconstructions of mid to late Holocene forest cover. These studies indicate that large-scale deforestation took place prior to the RP. For example, Yasuda et al. (2000) present evidence of deforestation in Syria as early as 9000 yr BP. A new semi-quantitative method for determining land cover from pollen percentages known as REVEALS (Regional Estimates of VEgetation Abundance from Large Sites) has shown that the largest anthropogenic changes in land cover in the Czech Republic took place between 3200–2700 yr BP (Mazier et al., 2010). In addition to empirical reconstructions, a number of models of human induced land cover change (Gaillard et al., 2010 for an overview) all indicate that extensive land clearance had occurred prior to the RP. Furthermore, we consider that the picture of the ancient Mediterranean landscape is open to misinterpretation. For instance, the city of Palmyra in modern Syria is presented as evidence of climatic aridification since the RP because this once flourishing city is now surrounded by desert (Huntington, 1911; Reale and Dirmeyer, 2000). However, Palmyra was established at an oasis (still present today) on an important trade route between the Western Levant and civilisations along the Tigris and Euphrates rivers. It was probably because of Palmyra's strategic location as a focal point of trade between kingdoms that it became such a large and prosperous city (Ortloff, 2005). In addition to the natural and historical archives, a recent study using a regional climate model simulation has indicated that precipitation in the Mediterranean region is insensitive to changes in land cover between potential vegetation and current landcover (Anav et al., 2010).

In order to determine whether the timing and extent of deforestation during the Late Holocene could have caused basin-wide climatic aridification around the Mediterranean, we incorporate maps of simulated preindustrial deforestation based on population estimates and technological advances (Kaplan et al., 2009) into climate simulations, using an Earth System model of Intermediate Complexity (EMIC). The outcomes of the simulations are interpreted in conjunction with a detailed analysis of the archaeological and historical record to understand if aridification trends between the RP and present existed, and were great enough to have affected humans. Changes in climatic humidity are inferred based on the distribution of archaeological sites in the Fertile Crescent in relation to present-day precipitation and land use. The analysis of ancient habitation distribution as a proxy of climate change is a novel approach that potentially allows for local-scale changes in rainfall distribution to be resolved.

## 2 Methodology

To identify the regional pattern of change in climatic humidity during the RP in the Mediterranean we perform an EOF analysis on a selection of high quality proxies of climatic humidity. We use model simulations to determine whether large-scale deforestation during the RP could have caused basin-wide climatic aridification in the Mediterranean, and imprinted on the signals of the proxies used in the EOF. An analysis of archaeological site distribution allows us to understand if aridification trends proposed to have occurred as a result of deforestation between the RP and present existed, and were great enough to have affected humans.

### 2.1 Reconstruction of precipitation around the Mediterranean

#### 2.1.1 Proxy records of climatic humidity

In total 12 proxy records of climatic humidity were used in our EOF analysis (Table 1). A search of the literature was carried out and each corresponding author contacted in order to access proxy data for analysis. In instances where authors were not contactable we digitised figures from the original papers using GetData software. Nine records were used from around the Mediterranean while a further three proxies of winter precipitation were added from Central and NW Europe, so that the signal in the Mediterranean proxies can be interpreted in the context of synoptic scale climate. The proxies in the Mediterranean are all records of annual changes in precipitation. However, because the Mediterranean receives the majority of its rainfall outside the summer months when precipitation is dominated by large-scale advection, we can assume that the variability in the Mediterranean proxies is primarily associated with variability of the synoptic regimes (Heck et al., 2001; Peel et al., 2007; Xoplaki et al., 2004). The proxies were selected according to three criteria. Firstly, we chose records with a maximum dating uncertainty of  $\pm 500$  yr so that millennial-scale climate changes during the 3000–1000 yr BP window of investigation are resolved and temporal changes can be compared. To ensure that climatic signals rather than noise associated with a proxy was compared; we used records with a proxy uncertainty less than the amplitude of change recorded in each respective time series during the period of the analysis. An additional requirement to perform an EOF analysis is that each record must cover the entire period of analysis. Based on these three criteria, a number of proxies of climatic humidity located around the Mediterranean were excluded from the analysis. Five records that satisfy the first two criteria but did not cover the entire period of analysis are included in the general discussion (Frogley et al., 2001; Jones et al., 2006; Marquer et al., 2008; Martín-Puertas et al., 2009; Orland et al., 2009).

#### 2.1.2 Empirical orthogonal function analysis of proxy records

An EOF analysis was used to identify the primary modes of variability among the 12 proxy records of climatic humidity. The EOF produces  $n$  modes of variability with the first  $k$  modes capturing most of the variability of the input dataset;  $n$  being the number of variables (i.e. proxy records used:  $n = 12$ ). The eigenvalue of each mode is a measure of the percentage of total variability explained by that mode. For those modes with high eigenvalues, the sign and magnitude of the loading values associated with each proxy illustrates the probable dominant patterns of change in climatic humidity between 3000 yr BP–1000 yr BP, recorded by the proxies used. Proxy time series with a large loading value in a certain mode have a larger contribution to the variability explained by that mode, compared with proxies with low loading values. If two proxy time series have opposing signs for their loading values it indicates that the time series of those proxies covary negatively in respect of the mode of variability under investigation. The principal component (PC),  $c_k$  of the  $k$ 'th mode of the EOF is given by:

$$c_k(t) = \sum_{i=1}^n x'(t, i) a_k(i). \quad (1)$$

Where  $x'$  is the detrended proxy time series,  $t$  is time,  $i$  is the proxy record,  $n$  are number of proxies,  $a_k(i)$  is the loading value of proxy  $i$  in the  $k$ 'th mode (Hannachi, 2004). Because we use only 12 input time series, it is important to test that the output statistics of the EOF are not affected by overfitting due to an outlier in the input dataset. To test for overfitting we applied a jack-knife resampling procedure. The jack-knife procedure was also used to determine which proxy records should be considered when interpreting the loading patterns in each mode of the EOF. Interpretation was confined to those records that decreased the average explained variability in each mode of the EOF when excluded from the jack-knife EOFs. The results of the jack-knife procedure and a more in-depth explanation of our statistical analyses is given in the Supplement.

Of the 12 proxy records used in the EOF each had differing sampling frequencies. In order that the comparison of variability in the EOF was based on equivalent frequencies of variation with noise reduced to a minimum, we derived a 1000 yr running mean for each record, following a linear interpolation of the original records to a consistent time interval. A 1000 yr running mean was deemed appropriate to facilitate meaningful comparisons among heterogeneous proxy records, whilst capturing millennial climate change during the period of analysis. In each case, the running mean for the period 3000–1000 yr BP was extracted from the running mean of the complete proxy time series. The running mean within 1000 yr of the beginning and end of the complete time series was scaled according to the number of years remaining. The running mean values were scaled to a common unit

**Table 1.** Proxy records of climatic humidity used as input in the empirical orthogonal function (EOF) analysis. The location of the proxy records is illustrated in Fig. 1

ID	Location	Proxy type	Dating uncertainty (years)	Reference
a	Norwegian Coast	Reconstructed glacier dynamics	±50	Bakke et al. (2008)
b	South West Norway	Reconstructed glacier dynamics	±60	Nesje et al. (2000)
c	West Central Alps	Reconstructed glacier dynamics	±200	Holzhauser et al. (2005)
d	Northern Spain	Oxygen Isotope ratios in speleothem	±150	Dominguez-villar et al. (2008)
e	North West Italy	Oxygen Isotope ratios in speleothem	±70	Zanchetta et al. (2007)
f	Central Italy	Reconstructed lake levels	±50	Magny et al. (2007)
g	South West Turkey	Stable isotope and pollen	±70	Eastwood et al. (2007)
h	Turkish Black Sea Coast	Uranium Isotope ratios in speleothem	±60	Göktürk et al. (2011)
i	Central Turkey	Stable isotope and pollen	±250	Roberts et al. (2001)
j	Dead Sea Israel	Reconstructed lake levels	±50	Bookman et al. (2004)
k	Dead Sea Israel	Reconstructed lake levels	±40	Migowski et al. (2006)
L	South East Turkey	Stable isotope and pollen	±500	Wick et al. (2003) and van Zeist and Woldring (1978) in Eastwood et al. (2007)

based on the amplitude of change in each record between 3000–1000 yr BP. These scaled running mean values were re-sampled into 200 time steps and used as input in the EOF. A plot of the running mean values overlaid on the respective proxy time series is supplied in the Supplement.

## 2.2 Isolation of anthropogenic signal

### 2.2.1 Deforestation simulation

Deforestation simulations were carried out at T42 spectral triangular resolution ( $\sim 2.8 \times 2.8$  degrees latitude-longitude) with 10 vertical layers using the Planet Simulator (PS), an EMIC with dynamic vegetation, mixed layer ocean capabilities and an Atmospheric General Circulation Model (AGCM) (Fraedrich et al., 2005a, b). Potential vegetation was derived by initialising the PS with a map of modern day above ground biomass (AGB) (Olson, 1983) and simulating 300 yr of dynamic vegetation growth until the biosphere had achieved equilibrium state (Dekker et al., 2010). Using model-derived AGB was deemed an appropriate method for an independent derivation of potential AGB for the Mediterranean, because although forest composition is known at different time periods at given sites, accurately estimating potential AGB for the entire Mediterranean from such records is difficult (Gaillard et al., 2010). Ancient deforestation was prescribed as a forested fraction of potential vegetation from 27.5° N to 55° N and 15° W to 50° E using maps of simulated deforestation based on population estimates and the contribution of technological advances (Kaplan et al., 2009).

Experiments were prescribed with climatologically derived, monthly SST averages for the period 1981–2002

(Reynolds et al., 2002). Each experiment lasted 30 yr, with the final 20 yr used in the analysis to ensure the system was at equilibrium with prescribed boundary conditions. We calculated the regional June–July–August (JJA) large-scale and convective precipitation (the contribution of vegetative evapotranspiration and other sources of precipitation) from the final 20 yr of simulations and adjusted the averaging at each cell to account for change in cell size at different latitudes. The spatially weighted values were averaged over all land cells from 27.5° N to 45° N and 10° W to 50° E to provide the regional JJA average and standard deviation of precipitation for the Mediterranean region. To understand how deforestation affected climate we compared 5 simulations: one of potential vegetation and four prescribed with a forested fraction of potential vegetation for time slices of 2500, 2000, 1500 and 100 yr BP (from Kaplan et al., 2009).

### 2.2.2 Archaeological site distribution as a proxy of aridification

The application of archaeological data as a proxy of climate change has precedent (Weiss et al., 1993), however, rather than focusing on one site we aim to understand changes in water availability in a wider context, with the analysis of the distribution of archaeological sites over the entire Fertile Crescent. The Fertile Crescent was chosen owing to the high density of archaeological sites and because previous studies indicate that precipitation reduced by half in the region, owing to deforestation since the RP (Reale and Shukla, 2000). Additionally, there are a number of modern studies that indicate that climate in parts of the Fertile Crescent is highly sensitive to changes in land cover (Alpert and

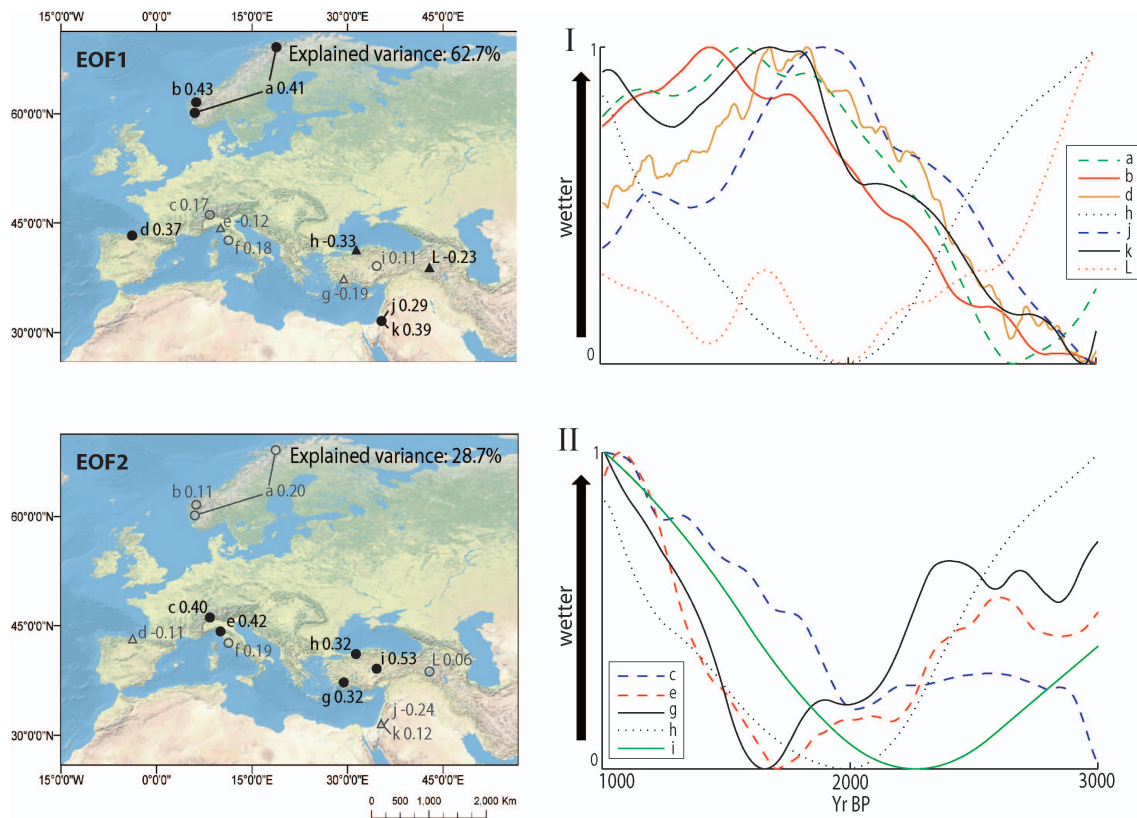


**Fig. 1.** Empirical Orthogonal Function analysis of 12 proxy indicators of climatic humidity. The maps display the geographic location of each proxy record and the associated loading values from EOF1 and EOF2 respectively. Circles and triangles indicate proxies which are anti-correlated in each mode. Records with the highest loadings are selected according to the criterion set out in Sect. 2.1.2. These are indicated by filled symbols whilst records with loading values below the selection threshold are indicated by hollow symbols. Panels I and II show the scaled 1000 yr running mean of the proxy time series with the highest loading values in each mode. Between 3000–1000 yr BP a wet-dry-wet fluctuation in climatic humidity is evident in the Central Mediterranean and Turkey while a dry-wet-dry fluctuation is indicated in Spain and Israel.

Mandel, 1986; De Ridder and Gallée, 1998). Given that the region is in a marginal climatic zone with steep gradients in precipitation over relatively short distances, it represents an ecotone between arable land and desert. Therefore, a trend towards aridification associated with deforestation will have caused the border of the ecotone to retreat, leaving previously occupied archaeological sites now abandoned in desert regions. Such a retreat of the arable ecotone occurred during the aridification event at 4200 yr BP (Weiss et al., 1993). By analysing the spatial distribution of archaeological sites in relation to the present arable ecotone, we can identify specific regions where climate may have become more arid since ancient times. It is important to note that archaeological site distribution in relation to the arable-desert ecotone can only capture an aridification trend indicated by the retreat of the arable ecotone. Stratigraphic analysis is required to identify the waxing and waning of the ecotone as Weiss et al. (1993) demonstrated at Tell Leilan.

Archaeological site data was provided from a georeferenced database of sites (Pedersen, 2010), dating from the Bronze Age until present. We used a gridded dataset of average yearly precipitation interpolated from rain gauge stations at 0.25 degree resolution for the period 1951–2007 (Yatagai et al., 2008) to determine present-day precipitation isohyets. Because this data is interpolated among rain gauges, the potential errors at each grid point varies depending on the spatiotemporal variation in rain gauge density around a grid point (Yatagai et al., 2008). Using ArcGIS 9, a 2 km buffer was placed around each site and a spatial analysis was done to determine whether a site coincided with agricultural or inhabited land (Tateishi et al., 2008). Visual inspection was carried out using Google Earth imagery and the Arc2Earth extension for ArcGIS.

### 3 Results

#### 3.1 Dominant modes of variability in precipitation

The maps of the loading patterns of the 1st two modes of the EOF analysis, explaining a combined 91.4 % of the variability in the 12 proxies used, are presented in Fig. 1. Plotted next to these maps are the running means of the scaled proxy time series. Only those time series that have the greatest contribution to the variability explained by EOF1 and EOF2 are plotted, according to the criterion set out in Sect. 2.1.2 (Fig. 1 I, II). A jack-knife resampling of the EOF procedure demonstrates that the EOF statistics are robust and not unduly influenced by an outlier proxy record (Supplement).

The map of the loading pattern of EOF1 (Fig. 1), accounting for 62.7 % of variability, displays positive correlation among two glacier records from Norway (a, b), one speleothem record from NW Spain (d) and two lake level records from the Dead Sea in Israel (j, k). These records are anti-correlated with one speleothem record (h) and one lake level record (L) from Turkey. The spatial pattern of the loadings from EOF1 indicates that the dominant change in climatic humidity during 3000–1000 yr BP was opposite between Turkey and the three other regions: Norway, NW Spain and Israel (NSI). Figure 1 (I) of the proxy time series shows that NSI exhibited a coincident increasing trend in climatic humidity from ca. 3000–1800 yr BP, followed by a decrease in climatic humidity of varying magnitude until 1000 yr BP. The Turkish proxies exhibit negative covariance with the time series of NSI and show an aridification trend from ca. 3000–2000 yr BP, followed by an increase in climatic humidity of varying magnitude until 1000 yr BP.

The map of the loading pattern of EOF2 (Fig. 1), accounting for 28.7 % of variability, displays positive correlation among a Glacier record from the West Central Alps (c), a speleothem record from NW Italy (e), two lake level records from Turkey (g, i) and one speleothem record from NW Turkey (h). Figure 1 (II) illustrates that these proxies exhibit a general trend towards drier conditions between ca. 3000–1800 yr BP. After ca. 1800 yr BP, all records exhibit a clear increase in climatic humidity. In general, the proxy records from The Alps, Italy and Turkey (AIT) exhibit negative covariance with NSI.

In each mode the trends towards increased precipitation at the beginning and end of the period of analysis represent the lower and upper limits respectively of the scaled running mean time series. This indicates that there is an overall wetting trend during the period of analysis among most of the proxies used (Fig. 1 I, II). The EOF is performed on detrended time series so the seesaw in climate indicated in our EOF is superimposed on this longer term wetting trend. The patterns exhibited by the EOF are consistent with a number of high resolution proxy time series from Spain, Tunisia, Greece, Turkey and Israel (Frogley et al., 2001; Jones et al., 2006; Marquer et al., 2008; Martín-Puertas

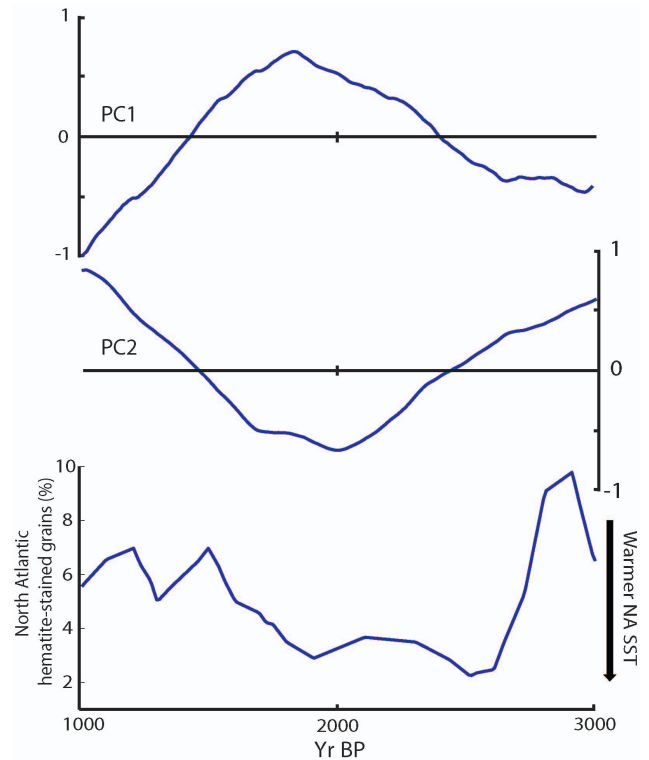


**Fig. 2.** The first two principal components (PCs) of 12 proxy records of climatic humidity (explaining a combined 91.4 % of variability) and a time series of ice rafted debris from the North Atlantic (Bond et al., 1997, 2001). The scale on the Y axis of the PC indices is dimensionless. Periods when the index of PC1 is highly positive coincide with wetter conditions in Norway, Spain and Israel. Periods when PC1 is highly negative coincide with wetter conditions in The Alps, Italy and Turkey.

et al., 2010; Orland et al., 2009). Although these proxies do not cover the entire period of analysis they demonstrate the same spatiotemporal signals as our EOF.

The detrended principal component (PC) time series of EOF1 and EOF2 are displayed in Fig. 2, along with the time series of the percentage of hematite-stained grains found in North Atlantic (NA) sediments during the period 3000–1000 yr BP (Bond et al., 1997, 2001). A higher percentage of hematite-stained grains are indicative of cooler winter SSTs in the North Atlantic. During Bond intervals when the percentage of hematite-stained grains is less and SST is warmer, the index of PC1 exhibits an increasing trend whilst PC2 exhibits a decreasing trend. During Bond events North Atlantic SSTs become cooler and the index of PC1 shifts to a negative trend whilst the index of PC2 takes on a positive trend. Given that the timing of changes in the PC time series are almost coincident, given that the PCs explain the majority of variability and because they are orthogonal, they are an index of the timing and magnitude of a seesaw in precipitation between AIT and NSI.

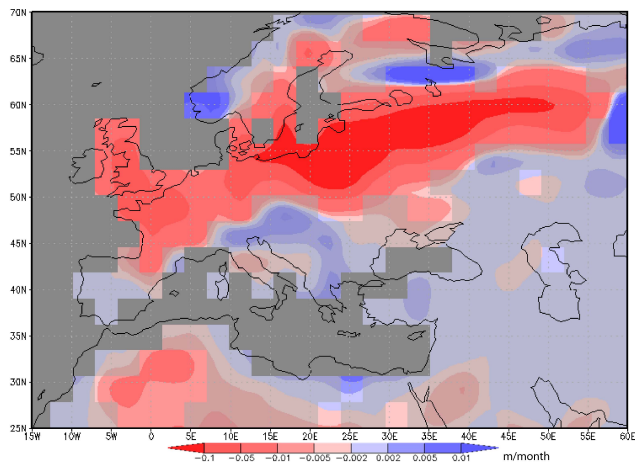


**Fig. 3.** Summer (JJA) average anomaly in precipitation ( $\text{m month}^{-1}$ ) for simulated forest cover at 100 yr BP minus potential forest cover. The largest changes in precipitation between potential forest cover and forest cover at 100 yr BP are in Northern Europe. The shaded areas are regions where the changes in precipitation are statistically insignificant ( $t(38) = 2.024$ ,  $p = 0.05$ ).

### 3.2 Impact of Deforestation on precipitation during the Roman Period

A map of the statistically significant ( $t(38) = 2.024$ ,  $p = 0.05$ ) anomaly in monthly mean JJA precipitation simulated by the PS between the situation of forest cover at 100 yr BP minus the situation with potential forest cover is presented in Fig. 3. It should be noted that the anomaly in terms of biomass between potential vegetation and vegetation at 100 yr BP is considerably less in the Mediterranean compared with Northern and Central Europe. This is owing to the low potential biomass simulated for the Mediterranean by the PS compared with AGB at northern latitudes. In our simulations, Northern and Western Europe exhibit significant (see non-shaded areas in Fig. 3) reductions in precipitation caused by deforestation. The simulated anomalies in JJA precipitation for these regions with very high anomalies in AGB are of similar magnitude to the present-day total average precipitation ( $>0.1 \text{ m month}^{-1}$ ). The Mediterranean region exhibits significant reductions in precipitation only in the Northern Morocco and Northern Spain.

Mean monthly JJA precipitation averaged over land cells in the Mediterranean region ( $27.5^\circ \text{ N}$  to  $45^\circ \text{ N}$  and  $10^\circ \text{ W}$  to  $50^\circ \text{ E}$ ) for simulations prescribed with potential AGB and AGB arising from deforestation (from Kaplan et al., 2000) at 2500, 2000, 1500 and 100 yr BP is presented in Fig. 4. The averaging includes arid regions such as the North Coast of Africa, hence the low monthly averages. No trend in precipitation is simulated as a result of decreased AGB for the 5 time slices shown. The differences among simulations are less than the “within simulation” standard deviation. Based on our simulations we conclude that deforestation in

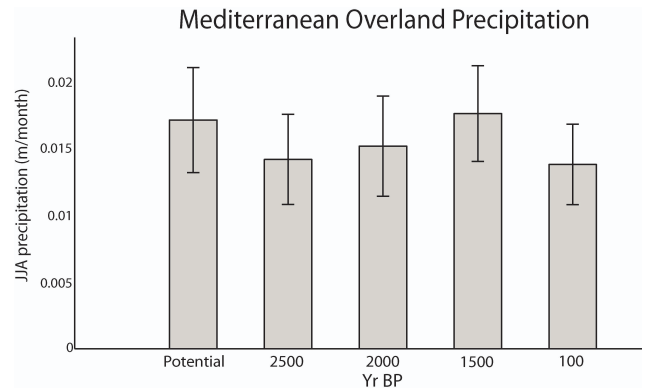


**Fig. 4.** Mediterranean summer (JJA) average overland precipitation ( $\text{m month}^{-1}$ ). The change in precipitation shown is in relation to land cover changes prescribed from Kaplan et al. (2009). Within simulation standard deviation is shown with error bars.

the Mediterranean was unlikely to have caused basin-wide aridification.

### 3.3 Archaeological site distribution in the Fertile Crescent

Archaeological site distribution in the Fertile Crescent in relation to present-day precipitation and arable land is presented in Fig. 5. The sites in green are those that coincide with currently inhabited or arable land. The sites in black are located neither on arable or inhabited land. In total 2345 sites were used in the analysis. Of these, 129 (5.5%) are now located in abandoned regions. The majority of abandoned sites are located along the North-East of the Jazira (A) and in lower Southern Mesopotamia (B). It can be seen that areas of arable land extend into regions that receive less than  $250 \text{ mm yr}^{-1}$  precipitation, which is considered the minimum requirement for dry-land farming (Bowden, 1979). In these regions, cultivation is possible, owing to the supplementation of precipitation in dry periods with irrigation from rainwater harvesting, wadi's (ephemeral streams), rivers and groundwater extraction; practices that were employed in ancient times as they are today (Huntington, 1911).

## 4 Discussion

The dominant pattern of variability between 3000–1000 yr BP depicted in our EOF analysis indicates a seesaw in climatic humidity in Europe with Norway, Spain and Israel (NSI) on one side and the Central Mediterranean and Turkey on the other (Fig. 1). In the Mediterranean, the seesaw in climatic humidity is expressed by a dry-wet-dry cycle in Spain and Israel, whilst a wet-dry-wet cycle occurred in the Central Mediterranean and Turkey. The timing of shifts in the seesaw is correlated with 1450 yr cycles in North Atlantic SST (Bond et al., 1997, 2001). The correlation between changes

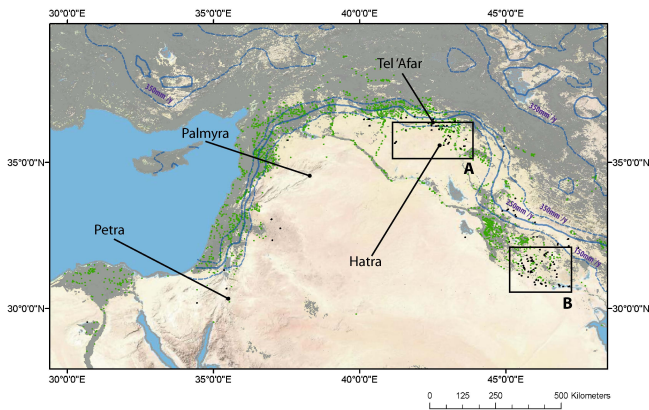


**Fig. 5.** Archaeological site distribution (Pedersen, 2010) overlaid with present-day precipitation and land cover. Green points are sites coinciding with land currently under cultivation or habitation, black points are sites in presently abandoned regions. Present-day precipitation is represented in isohyets and the grey region is land that is currently arable or inhabited. The regions marked A and B, where most of the abandoned sites are located, are in the North-East of the Jazira and lower Southern Mesopotamia respectively.

in climatic humidity and North Atlantic SST during the period of analysis is consistent with modern-day correlations between the position and intensity of the zonal jet stream and SST in the North Atlantic. Therefore, we propose that changes in climatic humidity over the Mediterranean during the RP were primarily caused by changes in the zonal jet streams associated with 1450 yr cycles in North Atlantic SST.

#### 4.1 Variability in Mediterranean precipitation during the Roman Period

The loading patterns of our EOF analysis illustrate an anti-correlation in climatic humidity between NSI and AIT during the period 3000–1000 yr BP (Fig. 1 I). NSI underwent a dry-wet-dry cycle between 3000–1000 yr BP whilst AIT exhibited an opposite wet-dry-wet signal during the same period (Fig. 1 I, II). A seesaw in climatic humidity between NSI and AIT is similar to the correlation in winter precipitation fields associated with the NAO index under present-day climate (Cullen and deMenocal, 2000; Hurrell, 1995). However, the positive correlation between Spain and Israel indicated in EOF1 is inconsistent with the present-day precipitation anomalies associated with NAO. In the Mediterranean a seesaw in climatic humidity between the Central Mediterranean and Turkey on one side and Spain and Israel on the other is consistent with precipitation anomalies associated with the East Atlantic/Western Russia pattern (EA/WR) (Barnston and Livezey, 1987; Dünkeloh and Jacobeit, 2003; Xoplaki et al., 2004). Therefore, we propose that the pattern for the whole of Europe during the RP is indicative of a superposition EA/WR and NAO-like patterns.

Support that the loading pattern in our EOF reflects a superposition of the NAO and EA/WR patterns is indicated by record (a) from Norway, which captures the gradient in winter precipitation between Northwest and Southwest Norway (Fig. 1i and Supplement). Periods when winter precipitation at both sites is at a maximum (minimum) indicate that the jet stream is at its northernmost (southernmost) extent and strongest (weakest) intensity. When the precipitation gradient between sites increases it represents an intermediate state of the jet stream (Bakke et al., 2008). The pattern indicated by the Norwegian Glacier records is consistent with present-day precipitation anomalies in Norway associated with coincident changes in the phases of the NAO and EA/WR (Krichak et al., 2002). Under coincident NAO+ and EA/WR+, a positive precipitation anomaly is seen along the entire west coast of Norway with the opposite case under NAO- and EA/WR-. When the NAO and EA/WR phases are opposite, the gradient in precipitation between North and South Norway is increased. In current climate the NAO is the dominant mode in this region, as positive precipitation anomalies in Norway only occur under NAO+ (Krichak et al., 2002). However, in the Mediterranean between 3000–1000 yr BP, the EA/WR pattern appears to be the dominant mode as the loading patterns in our EOF in the Mediterranean are consistent with correlations in the modern precipitation fields associated with the EA/WR pattern (Dünkeloh and Jacobeit, 2003; Xoplaki et al., 2004). Following Thompson and Wallace (1998), we thus propose that our proxies illustrate millennial shifts in the jet stream with NAO-like patterns, illustrating the meridional expression of these changes whilst in the Mediterranean the EA/WR-like patterns illustrate the zonal expression of changes in the jet stream (Enzel et al., 2003; Krichak et al., 2002). Therefore, we can conclude that the mechanism causing changes in precipitation over Europe during the RP are changes in the position and intensity of the jet stream. These changes are captured in modern climate by the AO index (Thompson and Wallace, 1998).

Whilst the EOF loading patterns illustrate regions of teleconnection in climatic humidity during 3000–1000 yr BP, the Principal Components (PCs) are an index of the timing and intensity of changes in climatic humidity in these regions. For example, periods when the index of PC1 (PC2) is highly positive (negative) are generally consistent with precipitation patterns associated with AO+ when the zonal jet streams are pushed northwards, and there is an increase in the intensity of the Polar Vortex (Thompson and Wallace, 1998). It can be seen in Fig. 2 that the timing of the shifts in the PC indices exhibit close correlation with the timing of cycles of ice-rafting events in the North Atlantic Ocean (Bond et al., 1997, 2001). During the Bond interval (ca. 2700–1800 yr BP), when North Atlantic winter SSTs were relatively warm, there was a trend towards wetter conditions in NSI indicated by a positive trend in PC1. The initiation of a period of cooler North Atlantic SSTs (ca. 1800 yr BP) coincided with a shift in the PC indices and a trend towards drier

conditions in NSI. The correlation between North Atlantic SST and the position and intensity of the jet stream indicated by our EOF is consistent with present-day correlations between the AO and North Atlantic SST. Therefore, we can tentatively conclude that changes in climatic humidity over the Mediterranean during the RP were primarily caused by a modification of the jet stream linked to SST change in the North Atlantic.

Changes in North Atlantic SST during Bond events have been linked to changes in the intensity of the Atlantic Meridional Overturning Circulation (AMOC) (Bond et al., 2001). Two important gradients relevant for AMOC intensity are the meridional gradient in SST between the equator and the poles, and the vertical density gradient in regions of the North Atlantic where Deep Water Formation (DWF) takes place. A decrease in either of these gradients is proposed to inhibit overturning circulation; therefore, causing a cooling in the North Atlantic (Wunsch, 2002). Various mechanisms are proposed to cause changes in these gradients (Dima and Lohmann, 2007; Krebs and Timmermann, 2007; Timmermann et al., 2007; Wang, 2007), with changes in the flux of fresh water to regions of DWF cited by a number of authors (Dickson et al., 1988; Fairbanks, 1989; Hurrell, 1995; Karcher et al., 2005; Polyakov and Johnson, 2000; Thornalley et al., 2009). Following Dima and Lohmann (2007), we propose that our study provides evidence that ocean-atmosphere coupling was an important factor in regulating AMOC during the period of analysis by modifying fresh water fluxes to regions of DWF in the North Atlantic. An increase in the northward atmospheric transport of fresh water during warm Bond intervals is shown in proxies (a) and (b), which are located close to regions of DWF in the North Atlantic (Bakke et al., 2008; Nesje et al., 2000). The increased atmospheric transport of fresh water to DWF regions during the Bond interval would have contributed to inhibiting deep water formation and a slowing down the AMOC thus cooling the North Atlantic. The cooling of the North Atlantic initiated a low phase of the AO and reduced northward transport of atmospheric fresh water thus promoting deep water formation. Given that we only capture one full 1450 yr cycle of a warm Bond interval and cool Bond event during our period of analysis we must be cautious with extrapolating over longer periods. However, our study indicates that ocean-atmosphere coupling provided a negative feedback to AMOC intensity that reduced surface salinity in North Atlantic DWF regions under high AMOC intensity, and increased it when AMOC intensity was low.

#### 4.2 Anthropogenic climate change during the Roman Period

We simulated the impact of ancient deforestation on Mediterranean precipitation in order to determine whether anthropogenic aridification associated with deforestation could

overprint the climatic signals in the proxies used in our EOF analysis. Our simulations indicated that precipitation in the Mediterranean at a basin-wide scale was probably insensitive to deforestation during the RP. Previous studies examining the basin-wide impact of deforestation on precipitation presented archaeological and historical evidence for large-scale aridification in the Eastern Mediterranean (Reale and Dirmeyer, 2000). However, our detailed analysis of the distribution of archaeological sites in the Fertile Crescent region in relation to present-day arable land showed no evidence of aridification since the RP.

##### 4.2.1 Impact of deforestation on precipitation

The finding that precipitation at a basin-wide scale around the Mediterranean was insensitive to deforestation is consistent with a recent regional climate model (RCM) study that found that the change from potential vegetation to current landcover had no effect on precipitation around the Mediterranean (Anav et al., 2010). Like our study, Anav et al. (2010) found that climate in Central and Northern Europe was most sensitive to changes in forest cover (Fig. 3). In our case we ascribe the difference in sensitivity of the Mediterranean and North/Central Europe primarily to the fact that the anomaly in AGB between potential vegetation and deforestation scenarios was much less in the Mediterranean compared with North/Central Europe, owing to the lower simulated potential vegetation particularly around the South Mediterranean. Lower biomass in these regions due to water stress is generally consistent with reality; however, because the resolution of our model cannot simulate detailed orography, some localised regions with higher elevations and thus higher annual rainfall are not captured by our simulations. It is possible therefore that individual proxy records in such regions may register feedbacks in climate, owing to deforestation in the period of analysis. Thus the use of many records using various types of proxies in our EOF analysis is noteworthy. The identification of spatially and temporally consistent patterns across a variety of proxy records gives us confidence that our interpretations are based on large-scale synoptic patterns, rather than locally heterogeneous feedbacks arising from anthropogenic activity.

##### 4.2.2 Archaeological evidence for climatic aridification?

The analysis of archaeological site distribution in the Fertile Crescent region in relation to present-day arable land found that 5.5 % of sites are in regions currently abandoned or too arid for viable habitation (Fig. 5). However, an understanding of the historical context of these sites is required before conclusions about climate based on their distribution can be made. Detailed historical descriptions of the North-Eastern Jazira region (Fig. 5a) exist from accounts of two Roman military campaigns in 177 AD and 363 AD. The site of Hatra,

which is currently in a desert region, is described by Cassius Dion (177 AD in Stein, 1941) as a city with “*neither water (save a small amount and that poor in quality) nor timber nor fodder. These very disadvantages, however, afford it protection, making impossible a siege by a large multitude*”. Hatra’s location in an arid region was quite typical of fortified cities from this era, but what such cities also had in common was that the groundwater table was high and could be exploited from wells within the city walls, thus making them almost impossible to besiege (Stein, 1941). A later account of the northward march of a Roman army from Hatra describes the crossing of an arid plain extending for 70 mille (110 km) which was void of potable water or edible vegetation as far as Ur (present-day Tel ‘Afar) (Ammianus Marcellinus, 363 AD in Stein, 1941). Tel ‘Afar today, as then, coincides with the northern border of the desert, indicating that the location of desert and arable ecotone has changed little since the RP in this region. The reason for a large number of abandoned sites between Hatra and Tel ‘Afar is that this plain is thought to have been an important trade route between kingdoms in lower Mesopotamia and those in the Northern Jazira plains: the route along the Tigris being too rugged for rapid movement (Ammianus Marcellinus, 363 AD in Stein, 1941). The abandoned sites along this route were located at springs (still present today) or where there was easy access to groundwater (Stein, 1941). Any site with even limited water supply in this arid plain could potentially profit as a focal point for trade on one of the busiest trade routes in the ancient world (Stein, 1941).

Lower Southern Mesopotamia (Fig. 5b) also exhibits a large number of abandoned sites. The extensive evidence for early irrigation in the Mesopotamian region suggests that in the past, as now, Mesopotamia received limited precipitation. Regions of Southern Mesopotamia were probably abandoned because, over time irrigation canals became clogged with sediment, owing to a breakdown in maintenance related to periods of political and social upheaval (Perry, 1986). Indeed many of the ancient, neglected irrigation canals in lower Mesopotamia are still visible from satellite imagery alongside abandoned archaeological sites in the dataset used (Pedersen, 2010). In fact, much of the region has only been brought back under irrigated cultivation in the latter half of the twentieth century (FAO, 2009). Therefore, the abandoned sites in lower Mesopotamia are not representative of change in climatic humidity; rather they demonstrate changes in land management over millennia. It could be argued therefore, that the sites in Southern Mesopotamia are not appropriate proxies of changing climatic humidity as agriculture in this region was always dependent on irrigation from the Tigris and Euphrates rivers. However, the establishment of early irrigation is indication in itself of persistent aridity in lower Mesopotamia from the beginnings of human civilisation in the mid Holocene.

Our archaeological analysis supports interpretations based on our simulations that no dramatic reductions in climatic

humidity occurred in the Fertile Crescent since the RP as a result of deforestation. Of course, conditions in the Fertile Crescent cannot be indicative of the entire Mediterranean. However, the detailed analysis of the archaeological record in a region of distinct ecotones that exhibit high climatic sensitivity to land cover change is instructive of the upper level of climatic sensitivity to deforestation that can be expected for the entire Mediterranean region. Therefore, we can be reasonably satisfied when making interpretations based on the signals captured in the EOF that the records are uninfluenced by basin-wide aridification caused by preindustrial anthropogenic climate change.

#### 4.3 The societal impact of climate change during the Roman Period

The climatic changes illustrated by our EOF analysis are indicative of the dominant millennial cycles in precipitation around the Mediterranean between 3000–1000 yr BP. However, as we have indicated these appear to overprint a longer term wetting trend among most of the proxies used. The cause of the wetting trend is not explored here; however, it indicates that the shift from dry to wet conditions in NSI and AIT in the first and second half of the period of analysis respectfully would have resulted in greater anomalies in precipitation than the shift from wet to dry in both regions. It is also important to realise that in many regions these shifts did not happen gradually as indicated by the smoothed time series used in our EOF but occurred quite suddenly. For instance the records of Jones et al. (2006) from Central Turkey and Bookman et al. (2004) from Israel illustrate sudden and dramatic shifts in climatic humidity of opposite directions between 1600–1400 yr BP (Supplement).

Shifts in climate, whether gradual or sudden, undoubtedly had an impact on agricultural productivity during the Roman Period and therefore on Roman society itself. However, the impact of climatic shifts on a society is dependent on how that society responds during benign or harsh climatic regimes (Blaikie and Brookfield, 1987; Diamond, 2005). For example, increasing agricultural intensity in marginal regions is demonstrated in Syria during the RP which brought about population increases, but also increased erosion and land degradation (Casana, 2008; Foss, 1997). The combination of population pressure and land degradation decreased societal resilience (Scheffer, 2009); nonetheless, population continued to grow until ca. 1400 yr BP, when a shift in climate appears to have been the trigger for widespread social upheaval in the region (Bookman et al., 2004; Foss, 1997; Jones et al., 2006). Whether the social upheaval in Syria ca. 1400 yr BP would have occurred with a different climate forcing or different societal behaviour is worthy of further research, particularly in the context of future climate change. Present societies are growing and degrading at unprecedented levels and risk eroding their resilience to deal with oscillations

in climate such as those associated with Bond events. These risks are compounded by the fact that natural oscillations can alternatively dampen the effects of anthropogenic climate change or be magnified by it.

## 5 Summary

Climate around the Mediterranean during the RP was typified by a millennial-scale seesaw in climatic humidity between Spain and Israel on one side and the Central Mediterranean and Turkey on the other. The patterns in climatic humidity are similar to precipitation anomalies associated with the East Atlantic/West Russia pattern in current climate (Barnston and Livezey, 1987; Krichak et al., 2002). In the period 3000–1000 yr BP, Spain and Israel underwent a dry-wet-dry cycle whilst a wet-dry-wet cycle occurred in the Central Mediterranean and Turkey. A model simulation indicates that the cycles of climatic humidity were unlikely to be influenced by climatic aridification caused by deforestation during the RP. That finding is supported by an analysis of the distribution of archaeological sites in the Fertile Crescent, which exhibits no evidence that human habitation distribution changed since ancient times as a result of climatic aridification.

The loading patterns of the first two modes of the EOF encompassing proxies from Northwest Europe and the Alps indicates that the climatic fluctuations in the Mediterranean were caused by millennial changes in the position of the jet stream and intensity of the polar vortex. The correlation between changes in North Atlantic SST and changes in the position and intensity of the jet stream indicated by our EOF is consistent with present-day correlations between the Arctic Oscillation and North Atlantic SST (Wallace, 2000). Therefore, we conclude that changes in climatic humidity over the Mediterranean during the RP were primarily caused by a modification of the jet stream linked to SST change in the North Atlantic (Bond et al., 1997, 2001). We tentatively propose that our findings indicate that ocean-atmosphere coupling may have contributed to a negative feedback in AMOC intensity during the period of analysis. Contextualizing long term climatic oscillations in terms of the Roman civilisation allows us to understand how such oscillations affect societal resilience. The interaction between climate oscillations and societal resilience is likely to become even more important in the future under unprecedented population growth and anthropogenic climate change (IPCC, 2007).

**Supplementary material related to this article is available online at:**  
<http://www.clim-past.net/8/637/2012/cp-8-637-2012-supplement.zip>.

*Acknowledgements.* The authors wish to thank Kaplan et al. (2009) for providing the digital data from their reconstruction of ancient deforestation. Thanks also go to Olof Pedersen who maintains an open-access database of archaeological sites in the Near East that was used in this project (Pedersen, 2010). We would also like to thank all the people who provided their proxy data for use in the EOF analysis. Finally thank you to two anonymous reviewers whose detailed and considered comments greatly improved the revised manuscript.

Edited by: D. Fleitmann

## References

- Alpert, P. and Mandel, M.: Wind Variability—An Indicator for a Mesoclimatic Change in Israel, *J. Appl. Meteorol.*, 25, 1568–1576, doi:10.1175/1520-0450(1986)025<1568:WVIFAM>2.0.CO;2, 1986.
- Anav, A., Ruti, P. M., Artale, V. and Valentini, R.: Modelling the effects of land-cover changes on surface climate in the Mediterranean region, *Clim. Res.*, 41, 91–104, doi:10.3354/cr00841, 2010.
- Bakke, J., Lie, Ø., Dahl, S. O., Nesje, A., and Bjune, A. E.: Strength and spatial patterns of the Holocene wintertime westerlies in the NE Atlantic region, *Global Planet. Change*, 60, 28–41, 2008.
- Baldwin, M. P. and Dunkerton, T. J.: Propagation of the Arctic Oscillation from the stratosphere to the troposphere, *J. Geophys. Res.*, 104, 30937–30946, doi:10.1029/1999JD900445, 1999.
- Barnston, A. and Livezey, R.: Classification, seasonality and persistence of low-frequency atmospheric circulation patterns, *Mon. Weather Rev.*, 115, 1083–1126, 1987.
- Bianchi, G. G. and McCave, I. N.: Holocene periodicity in North Atlantic climate and deep-ocean flow south of Iceland, *Nature*, 397, 515–517, doi:10.1038/17362, 1999.
- Blaikie, P. M. and Brookfield, H. C.: *Land degradation and society*, Taylor & Francis, 1987.
- Bond, G., Showers, W., Cheseby, M., Lotti, R., Almasi, P., deMenocal, P., Priore, P., Cullen, H., Hajdas, I., and Bonani, G.: A Pervasive Millennial-Scale Cycle in North Atlantic Holocene and Glacial Climates, *Science*, 278, 1257–1266, doi:10.1126/science.278.5341.1257, 1997.
- Bond, G., Kromer, B., Beer, J., Muscheler, R., Evans, M. N., Showers, W., Hoffmann, S., Lotti-Bond, R., Hajdas, I., and Bonani, G.: Persistent solar influence on North Atlantic climate during the Holocene, *Science*, 294, 2130, doi:10.1126/science.1065680, 2001.
- Bookman, R., Enzel, Y., Agnon, A., and Stein, M.: Late Holocene lake levels of the Dead Sea, *Geol. Soc. Am. Bull.*, 116, 555–571, doi:10.1130/B25286.1, 2004.
- Bowden L.: *Development of Present Dryland Farming Systems in: Agriculture in semi-arid environments*, edited by: Hall, A. E., Cannell, G. H., and Lawton, H. W., Springer Verlag, 1979.
- Brovkin, V., Claussen, M., Petoukhov, V., and Ganopolski, A.: On the stability of the atmosphere-vegetation system in the Sahara/Sahel region, *J. Geophys. Res.*, 103, 31613–31624, doi:10.1029/1998JD200006, 1998.
- Büntgen, U., Tegel, W., Nicolussi, K., McCormick, M., Frank, D., Trouet, V., Kaplan, J. O., Herzig, F., Heussner, K.-U., Wanner,

- H., Luterbacher, J., and Esper, J.: 2500 Years of European Climate Variability and Human Susceptibility, *Science*, 331, 578–582, doi:10.1126/science.1197175, 2011.
- Casana, J.: Mediterranean valleys revisited: Linking soil erosion, land use and climate variability in the Northern Levant, *Geomorphology*, 101, 429–442, doi:10.1016/j.geomorph.2007.04.031, 2008.
- Charney, J., Stone, P. H., and Quirk, W. J.: Drought in the Sahara: A Biogeophysical Feedback Mechanism, *Science*, 187, 434–435, doi:10.1126/science.187.4175.434, 1975.
- Cohen, J. and Jones, J.: Tropospheric precursors and stratospheric warmings, *J. Climate*, 24, 6562–6572, 2011.
- Cook, E. R., D'Arrigo, R. D., and Mann, M. E.: A well-verified, multiproxy reconstruction of the winter North Atlantic Oscillation Index since ad 1400\*, *J. Climate*, 15, 1754–1764, 2002.
- Cullen, H. M. and deMenocal, P. B.: North Atlantic influence on Tigris-Euphrates streamflow, *Int. J. Climatol.*, 20, 853–863, doi:10.1002/1097-0088(20000630)20:8<853::AID-JOC497>3.0.CO;2-M, 2000.
- Dekker, S. C., de Boer, H. J., Brovkin, V., Fraedrich, K., Wassen, M. J., and Rietkerk, M.: Biogeophysical feedbacks trigger shifts in the modelled vegetation-atmosphere system at multiple scales, *Biogeosciences*, 7, 1237–1245, doi:10.5194/bg-7-1237-2010, 2010.
- Desprat, S., Sánchez Goñi, M. F., and Loutre, M.-F.: Revealing climatic variability of the last three millennia in northwestern Iberia using pollen influx data, *Earth Planet. Sci. Lett.*, 213, 63–78, doi:10.1016/S0012-821X(03)00292-9, 2003.
- Diamond, J.: *Collapse: How Societies Choose to Fail Or Succeed*, Penguin Group USA, New York, USA, 2005.
- Dickson, R. R., Meincke, J., Malmberg, S. A., and Lee, A. J.: The great salinity anomaly in the northern North Atlantic 1968–1982, *Prog. Oceanogr.*, 20, 103–151, 1988.
- Dima, M. and Lohmann, G.: A hemispheric mechanism for the Atlantic Multidecadal Oscillation, *J. Climate*, 20, 2706–2719, 2007.
- Dominguez-villar, D., Wang, X., Cheng, H., Martinchivelet, J., and Edwards, R.: A high-resolution late Holocene speleothem record from Kaithe Cave, northern Spain:  $\delta^{18}\text{O}$  variability and possible causes, *Quatern. Int.*, 187, 40–51, doi:10.1016/j.quaint.2007.06.010, 2008.
- Düinkeloh, A. and Jacobeit, J.: Circulation dynamics of Mediterranean precipitation variability 1948–98, *Int. J. Climatol.*, 23, 1843–1866, doi:10.1002/joc.973, 2003.
- Dümenil Gates, L. and Ließ, S.: Impacts of deforestation and afforestation in the Mediterranean region as simulated by the MPI atmospheric GCM, *Global Planet. Change*, 30, 309–328, doi:10.1016/S0921-8181(00)00091-6, 2001.
- Eastwood, W. J., Leng, M. J., Roberts, N., and Davis, B.: Holocene climate change in the eastern Mediterranean region: a comparison of stable isotope and pollen data from Lake Gölhisar, southwest Turkey, *J. Quaternary Sci.*, 22, 327–341, doi:10.1002/jqs.1062, 2007.
- Enzel, Y., Bookman (Ken Tor), R., Sharon, D., Gvirtzman, H., Dayan, U., Ziv, B., and Stein, M.: Late Holocene climates of the Near East deduced from Dead Sea level variations and modern regional winter rainfall, *Quaternary Res.*, 60, 263–273, doi:10.1016/j.yqres.2003.07.011, 2003.
- Erdkamp, P.: The grain market in the Roman Empire: a social, political and economic study, Cambridge University Press, 2005.
- Fairbanks, R. G.: A 17,000-year glacio-eustatic sea level record: influence of glacial melting rates on the Younger Dryas event and deep-ocean circulation, *Nature*, 342, 637–642, 1989.
- FAO: Irrigation in the Middle East region in figures, Survey, Food and Agriculture Organisation of the United Nations, Rome, 2009.
- Fleitmann, D., Burns, S. J., Mudelsee, M., Neff, U., Kramers, J., Mangini, A., and Matter, A.: Holocene Forcing of the Indian Monsoon Recorded in a Stalagmite from Southern Oman, *Science*, 300, 1737–1739, doi:10.1126/science.1083130, 2003.
- Foss, C.: Syria in Transition, A. D. 550–750: An Archaeological Approach, *Dumbarton Oaks Papers*, 51, 189–269, 1997.
- Fraedrich, K., Jansen, H., Kirk, E., Luksch, U., and Lunkeit, F.: The Planet Simulator: Towards a user friendly model, *Meteorol. Z.*, 14, 299–304, doi:10.1127/0941-2948/2005/0043, 2005a.
- Fraedrich, K., Jansen, H., Kirk, E., and Lunkeit, F.: The Planet Simulator: Green planet and desert world, *Meteorol. Z.*, 14, 305–314, doi:10.1127/0941-2948/2005/0044, 2005b.
- Frogley, M. R., Griffiths, H. I., and Heaton, T. H. E.: Historical Biogeography and Late Quaternary Environmental Change of Lake Pamvotis, Ioannina (North-Western Greece): Evidence from Ostracods, *J. Biogeogr.*, 28, 745–756, 2001.
- Gaillard, M.-J., Sugita, S., Mazier, F., Trondman, A.-K., Broström, A., Hickler, T., Kaplan, J. O., Kjellström, E., Kokfelt, U., Kunes, P., Lemmen, C., Miller, P., Olofsson, J., Poska, A., Rundgren, M., Smith, B., Strandberg, G., Fyfe, R., Nielsen, A. B., Aleinius, T., Balakauskas, L., Barnekow, L., Birks, H. J. B., Bjune, A., Björkman, L., Giesecke, T., Hjelle, K., Kalnina, L., Kangur, M., van der Knaap, W. O., Koff, T., Lagerßs, P., Latałowa, M., Leydet, M., Lechterbeck, J., Lindbladh, M., Odgaard, B., Peglar, S., Segerström, U., von Stedingk, H., and Seppä, H.: Holocene land-cover reconstructions for studies on land cover-climate feedbacks, *Clim. Past*, 6, 483–499, doi:10.5194/cp-6-483-2010, 2010.
- Göktürk, O. M., Fleitmann, D., Badertscher, S., Cheng, H., Edwards, R. L., Leuenberger, M., Fankhauser, A., Tüysüz, O., and Kramers, J.: Climate on the southern Black Sea coast during the Holocene: implications from the Sofular Cave record, *Quaternary Sci. Rev.*, 30, 2433–2445, doi:10.1016/j.quascirev.2011.05.007, 2011.
- Hannachi, A.: A primer for EOF analysis of climate data, Department of Meteorology, University of Reading, 2004.
- Heck, P., Lüthi, D., Wernli, H. and Schär, C.: Climate impacts of European-scale anthropogenic vegetation changes: A sensitivity study using a regional climate model, *J. Geophys. Res.*, 106, 7817–7835, doi:10.1029/2000JD900673, 2001.
- Holzhauser, H., Magny, M., and Zumbühl, H. J.: Glacier and lake-level variations in west-central Europe over the last 3500 years, *The Holocene*, 15, 789–801, doi:10.1191/0959683605hl853ra, 2005.
- Horden, P. and Purcell, N.: *The corrupting sea: a study of Mediterranean history*, Wiley-Blackwell, 2000.
- Huntington, E.: *Palestine and its transformation*, Houghton Mifflin company, 1911.
- Hurrell, J. W.: Decadal Trends in the North Atlantic Oscillation: Regional Temperatures and Precipitation, *Science*, 269, 676–679, doi:10.1126/science.269.5224.676, 1995.
- IPCC AR4 SYR, Core Writing Team, Pachauri, R. K., and

- Reisinger, A. (Ed.): *Climate Change 2007: Synthesis Report, Contribution of Working Groups I, II and III to the Fourth Assessment Report of the Intergovernmental Panel on Climate Change*, IPCC, ISBN 92-9169-122-4, 2007.
- Issar, A. S. and Yakir, D.: Isotopes from Wood Buried in the Roman Siege Ramp of Masada: The Roman Period's Colder Climate, *The Biblical Archaeologist*, 60, 101, doi:10.2307/3210599, 1997.
- Jones, M. D., Roberts, C. N., Leng, M. J., and Türke, M.: A high-resolution late Holocene lake isotope record from Turkey and links to North Atlantic and monsoon climate, *Geol.*, 34, 361, doi:10.1130/G22407.1, 2006.
- Kaplan, J., Krumhardt, K., and Zimmermann, N.: The prehistoric and preindustrial deforestation of Europe, *Quaternary Sci. Rev.*, 28, 3016–3034, doi:10.1016/j.quascirev.2009.09.028, 2009.
- Karcher, M., Gerdes, R., Kauker, F., Köberle, C., and Yashayaev, I.: Arctic Ocean change heralds North Atlantic freshening, *Geophys. Res. Lett.*, 32, 1–5, 2005.
- Krebs, U. and Timmermann, A.: Tropical air-sea interactions accelerate the recovery of the Atlantic meridional overturning circulation after a major shutdown, *J. Climate*, 20, 4940–4956, 2007.
- Krichak, S. O., Kishcha, P., and Alpert, P.: Decadal trends of main Eurasian oscillations and the Eastern Mediterranean precipitation, *Theor. Appl. Climatol.*, 72, 209–220, doi:10.1007/s007040200021, 2002.
- Magny, M., de Beaulieu, J.-L., Drescher-Schneider, R., Vanni re, B., Walter-Simonnet, A.-V., Miras, Y., Millet, L., Bossuet, G., Peyron, O., Brugiapaglia, E., and Leroux, A.: Holocene climate changes in the central Mediterranean as recorded by lake-level fluctuations at Lake Accesa (Tuscany, Italy), *Quaternary Sci. Rev.*, 26, 1736–1758, doi:10.1016/j.quascirev.2007.04.014, 2007.
- Marquer, L., Pomel, S., Abichou, A., Schulz, E., Kaniewski, D., and Van Campo, E.: Late Holocene high resolution palaeoclimatic reconstruction inferred from Sebkhah Mhabeul, southeast Tunisia, *Quaternary Res.*, 70, 240–250, doi:10.1016/j.yqres.2008.06.002, 2008.
- Mart n-Puertas, C., Valero-Garc s, B. L., Brauer, A., Mata, M. P., Delgado-Huertas, A. and Dulski, P.: The Iberian-Roman Humid Period (2600–1600 cal yr BP) in the Zo nar Lake varve record (Andaluc a, southern Spain), *Quaternary Res.*, 71, 108–120, doi:10.1016/j.yqres.2008.10.004, 2009.
- Mart n-Puertas, C., Jim nez-Espejo, F., Mart nez-Ruiz, F., Nieto-Moreno, V., Rodrigo, M., Mata, M. P., and Valero-Garc s, B. L.: Late Holocene climate variability in the southwestern Mediterranean region: an integrated marine and terrestrial geochemical approach, *Clim. Past*, 6, 807–816, doi:10.5194/cp-6-807-2010, 2010.
- Mayewski, P. A., Rohling, E. E., Curt Stager, J., Karl n, W., Maasch, K. A., David Meeker, L., Meyerson, E. A., Gasse, F., van Kreveld, S., Holmgren, K., Lee-Thorp, J., Rosqvist, G., Rack, F., Staubwasser, M., Schneider, R. R., and Steig, E. J.: Holocene climate variability, *Quaternary Res.*, 62, 243–255, doi:10.1016/j.yqres.2004.07.001, 2004.
- Mazier, F., Kuneš, P., Sugita, S., Trondman, A.-K., Brostr m, A., and Gaillard, M.-J.: Pollen-inferred quantitative reconstructions of Holocene land-cover in NW Europe for the evaluation of past climate-vegetation feedbacks -Evaluation of the REVEALS-based reconstruction using the Czech Republic database, available at: <http://adsabs.harvard.edu/abs/2010EGUGA..12.4248M>, last access: 11 November 2010, 2010.
- Migowski, C., Stein, M., Prasad, S., Negendank, J. F. W., and Agnon, A.: Holocene climate variability and cultural evolution in the Near East from the Dead Sea sedimentary record, *Quaternary Res.*, 66, 421–431, doi:10.1016/j.yqres.2006.06.010, 2006.
- Namias, J.: The index cycle and its role in the general circulation., *J. Atmos. Sci.*, 7, 130–139, 1950.
- Nesje, A., Lie,  ., and Dahl, S. O.: Is the North Atlantic Oscillation reflected in Scandinavian glacier mass balance records?, *J. Quaternary Sci.*, 15, 587–601, doi:10.1002/1099-1417(200009)15:6<587::AID-JQS533>3.0.CO;2-2, 2000.
- Olson, J. S., Watts, J. A., and Allison L. J.: *Carbon in Live Vegetation of Major World Ecosystems*, Oak Ridge, TN: Oak Ridge National Laboratory, 1983.
- Orland, I., Barmathews, M., Kita, N., Ayalon, A., Matthews, A., and Valley, J.: Climate deterioration in the Eastern Mediterranean as revealed by ion microprobe analysis of a speleothem that grew from 2.2 to 0.9 ka in Soreq Cave, Israel, *Quaternary Res.*, 71, 27–35, doi:10.1016/j.yqres.2008.08.005, 2009.
- Ortloff, C. R.: The Water Supply and Distribution System of the Nabataean City of Petra (Jordan), 300 BC– AD 300, *Camb. Archaeol. J.*, 15, 93–109, doi:10.1017/S0959774305000053, 2005.
- Pedersen, O.: Ancient near east sites on google earth, [available at: <http://www.anst.uu.se/olofpede/Links.htm>, last access: 20 October 2010, 2010.
- Peel, M. C., Finlayson, B. L., and McMahon, T. A.: Updated world map of the K ppen-Geiger climate classification, *Hydrol. Earth Syst. Sci.*, 11, 1633–1644, doi:10.5194/hess-11-1633-2007, 2007.
- Perry, R. A.: Desertification processes and impacts in irrigated regions, *Climatic Change*, 9, 43–47, doi:10.1007/BF00140523, 1986.
- Polyakov, I. V. and Johnson, M. A.: Arctic decadal and interdecadal variability, *Geophys. Res. Lett.*, 27, 4097–4100, doi:10.1029/2000GL011909, 2000.
- Reale, O. and Dirmeyer, P.: Modeling the effects of vegetation on Mediterranean climate during the Roman Classical Period: Part I: Climate history and model sensitivity, *Global Planet. Change*, 25, 163–184, doi:10.1016/S0921-8181(00)00002-3, 2000.
- Reale, O. and Shukla, J.: Modeling the effects of vegetation on Mediterranean climate during the Roman Classical Period: Part II. Model simulation, *Global Planet. Change*, 25, 185–214, doi:10.1016/S0921-8181(00)00003-5, 2000.
- Reynolds, R. W., Rayner, N. A., Smith, T. M., Stokes, D. C., and Wang, W.: An improved in situ and satellite SST analysis for climate, *J. Climate*, 15, 1609–1625, 2002.
- De Ridder, K. and Gall e, H.: Land Surface-Induced Regional Climate Change in Southern Israel, *J. Appl. Meteor.*, 37, 1470–1485, doi:10.1175/1520-0450(1998)037<1470:LSIRCC>2.0.CO;2, 1998.
- Rimbu, N., Lohmann, G., Kim, J.-H., Arz, H. W., and Schneider, R.: Arctic/North Atlantic Oscillation signature in Holocene sea surface temperature trends as obtained from alkenone data, *Geophys. Res. Lett.*, 30, 1280–1283, doi:10.1029/2002GL016570, 2003.
- Roberts, N., Reed, J. M., Leng, M. J., Kuzucuolu, C., Fontugne, M., Bertaux, J., Woldring, H., Bottema, S., Black, S., Hunt, E., and Karabiyyikolu, M.: The tempo of Holocene climatic change

- in the eastern Mediterranean region: new high-resolution crater-lake sediment data from central Turkey, *The Holocene*, 11, 721–736, doi:10.1191/09596830195744, 2001.
- Scheffer, M.: *Critical transitions in nature and society*, Princeton University Press., 2009.
- Stein, A.: The Ancient Trade Route Past Hatra and Its Roman Posts, *J. Roy. Asiatic Soc. Great Britain and Ireland*, 4, 299–316, 1941.
- Tateishi, R., Bayer, M., Ghar, A., and Al-Bilbisi, H.: A New Global Land Cover Map (GLCNMO), ISPRS, 2008.
- Thompson, D. W. J. and Wallace, J. M.: The Arctic oscillation signature in the wintertime geopotential height and temperature fields, *Geophys. Res. Lett.*, 25, 1297, doi:10.1029/98GL00950, 1998.
- Thornalley, D. J. R., Elderfield, H., and McCave, I. N.: Holocene oscillations in temperature and salinity of the surface subpolar North Atlantic, *Nature*, 457, 711–714, doi:10.1038/nature07717, 2009.
- Timmermann, A., Okumura, Y., An, S. I., Clement, A., Dong, B., Guilyardi, E., Hu, A., Jungclaus, J., Renold, M., Stocker, T., Stouffer, R. J., Sutton, R., Xie, S.-P., and Yin, J.: The influence of a weakening of the Atlantic meridional overturning circulation on ENSO, *J. Climate*, 20, 4899–4919, 2007.
- Trouet, V., Esper, J., Graham, N. E., Baker, A., Scourse, J. D., and Frank, D. C.: Persistent Positive North Atlantic Oscillation Mode Dominated the Medieval Climate Anomaly, *Science*, 324, 78–80, doi:10.1126/science.1166349, 2009.
- van Zeist, W. and Woldring, H.: A Postglacial pollen diagram from Lake Van in East Anatolia, *Rev. Palaeobot. Palyno.*, 26, 249–276, 1978.
- Wallace, J.: On the Arctic and Antarctic oscillations, in *Proceedings of the 23rd Annual Climate. Diagnostics and Prediction workshop*, NOAA, NWS, Department of Commerce, Florida, USA, available at: [http://www.jisao.washington.edu/wallace/ncar\\_notes/](http://www.jisao.washington.edu/wallace/ncar_notes/), last access: 1 December 2011, 2000.
- Wang, C.: Variability of the Caribbean low-level jet and its relations to climate, *Clim. Dynam.*, 29, 411–422, 2007.
- Weiss, H., Courty, M.-A., Wetterstrom, W., Guichard, F., Senior, L., Meadow, R., and Curnow, A.: The Genesis and Collapse of Third Millennium North Mesopotamian Civilization, *Science*, 261, 995–1004, doi:10.1126/science.261.5124.995, 1993.
- Wick, L., Lemcke, G., and Sturm, M.: Evidence of Lateglacial and Holocene climatic change and human impact in eastern Anatolia: high-resolution pollen, charcoal, isotopic and geochemical records from the laminated sediments of Lake Van, Turkey, *The Holocene*, 13, 665–675, doi:10.1191/0959683603hl653rp, 2003.
- Wunsch, C.: What Is the Thermohaline Circulation?, *Science*, 298, 1179–1181, doi:10.1126/science.1079329, 2002.
- Xoplaki, E., Gonzalez-Rouco, J. F., Luterbacher, J., and Wanner, H.: Wet season Mediterranean precipitation variability: influence of large-scale dynamics and trends, *Clim. Dynam.*, 23, 63–78, 2004.
- Yasuda, Y., Kitagawa, H., and Nakagawa, T.: The earliest record of major anthropogenic deforestation in the Ghab Valley, northwest Syria: a palynological study, *Quaternary Int.*, 73–74, 127–136, doi:10.1016/S1040-6182(00)00069-0, 2000.
- Yatagai, A., Xie, P., and Alpert, P.: Development of a daily gridded precipitation data set for the Middle East, available at: <http://hal.archives-ouvertes.fr/hal-00297073/en/>, last access: 7 January 2011, 2008.
- Zanchetta, G., Drysdale, R. N., Hellstrom, J. C., Fallick, A. E., Isola, I., Gagan, M. K., and Pareschi, M. T.: Enhanced rainfall in the Western Mediterranean during deposition of sapropel S1: stalagmite evidence from Corchia cave (Central Italy), *Quaternary Sci. Rev.*, 26, 279–286, doi:10.1016/j.quascirev.2006.12.003, 2007.
- Zhang, H. and Oweis, T.: Water–yield relations and optimal irrigation scheduling of wheat in the Mediterranean region, *Agr. Water Manage.*, 38, 195–211, doi:10.1016/S0378-3774(98)00069-9, 1999.
- Ziv, B., Dayan, U., Kushnir, Y., Roth, C., and Enzel, Y.: Regional and global atmospheric patterns governing rainfall in the southern Levant, *Int. J. Climatol.*, 26, 55–73, doi:10.1002/joc.1238, 2006.